Macromolecules

ARTICLE

pubs.acs.org/Macromolecules

Mesogen-Initiated Linear Polyglycerol Isomers: The Ordering Effect of a Single Cholesterol Unit on "Sticky" Isotropic Chains

Anna Maria Hofmann,[†] Robert Wipf,[‡] Bernd Stühn,[*,‡] and Holger Frey[*,†]

[†]Institut für Organische Chemie, Johannes Gutenberg-Universität, Duesbergweg 10-14, 55099 Mainz, Germany

[‡]Institut für Festkörperphysik, Technische Universität Darmstadt, Hochschulstrasse 8, 64289 Darmstadt, Germany

Supporting Information

ABSTRACT: Synthesis, thermal properties, and the liquid crystalline (LC) order of polymers consisting of a single mesogenic cholesterol unit and flexible, linear polyglycerol (PG) or poly(glyceryl glycerol) (PGG) chains have been investigated. Incorporation of the single mesogen has been achieved by using cholesterol directly as an initiator for the oxyanionic ring-opening polymerization (ROP) of ethoxyethyl glycidyl ether (EEGE) or isopropylidene glyceryl glycidyl ether (IGG). The controlled polymerization allowed the synthesis of a series of peculiar rod−coil type polyethers with molecular weights of 600−2300 g/mol, representing a degree of polymerization (DP_n) of 4−30 for both PG and PGG with the polydispersity M_w/M_n in the range of 1.07−1.25. The resulting linear PGs exhibit extremely stable thermotropic LC order in a broad temperature range up to 260 °C, forming mainly layered smectic A (SmA) phases with varying layer thicknesses, depending on the degree of polymerization of the respective polymer structure. LC phases were observed up to a chain length of 26 glycerol units, while PGGs showed no LC order. This is explained both by the steric hindrance of the branched monomer units and the higher hydrophilicity of the polymer backbone. Permethylation of the cholesterol-PG samples resulted in strongly reduced LC order or in the entire loss of the self-assembly in LC phases, which is a consequence of the disappearance of hydrogen-bonding between the functional coil segments. Detailed characterization of the phase behavior of the polymers has been achieved by differential scanning calorimetry (DSC), polarized optical microscopy (POM), and small-angle X-ray scattering (SAXS), confirming the smectic layer structure of the materials.

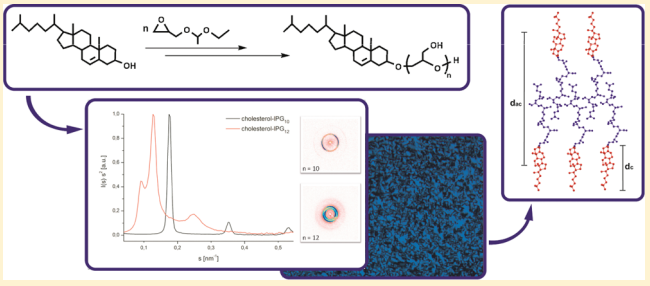

INTRODUCTION

Self-assembly in thermotropic liquid crystalline (LC) phases has been long known for cholesterol-derived compounds. In fact, the first observation of LC phases ever was made for cholesteryl benzoates and cholesteryl acetates.[1] The functionalization of dendrimers and polymers with cholesterol or other mesogenic moieties is a common strategy for the preparation of unusual types of LC materials.[2−4] Both main-chain and side-chain type LC dendrimers, in which the mesogenic moieties are grafted onto functional groups in the periphery of the preformed precursor, have been reported.[5−11] A large variety of side-chain LC polymers based on various polymer scaffolds, such as linear poly(ethylene glycol) (PEG), poly(DL-lactide) (P-DL-LA), polyacrylates, hyperbranched polyglycerol (*hb*PG), or poly(*p*-chloromethylstyrene) and others, has been prepared by polymer modification with cholesterol groups.[12−18] LC polymers with cholesterol moieties have also been prepared by the polymerization of monomers containing mesogenic moieties such as cholesterol-based epoxides or cholesteryl methacrylates.[19,20]

In pronounced contrast to polymers bearing multiple mesogens, in only few cases the terminal functionalization of polymer chains with a single mesogen has been achieved by using these directly for the initiation of polymerizations, namely, for several polyester structures, such as poly(L-lactid acid), poly(trimethylene carbonate) (PTMC), poly(ε-caprolactone) (PCL), and poly(lactide-*co*-glycolide) (PLG).[21−24] In all cases LC phases are formed by self-assembly of the mesogen-initiated oligomers in neat state, such as smectic phases at elevated temperatures for the cholesteryl end-capped oligo(L-lactic acid).

To the best of our knowledge, the incorporation of mesogens in polymers using the respective mesogenic molecule directly as an initiator for the anionic or oxyanionic polymerization has not been reported to date. In the present study polyglycerols with varied molecular architectures have been synthesized via oxyanionic ring-opening polymerization (ROP) of different glycidyl ether monomers, that is, ethoxyethyl glycidyl ether (EEGE)[25−28] and isopropylidene glyceryl glycidyl ether (IGG) (Figure 1).[25,26,29−36] Direct initiation of the polymerizations with deprotonated cholesterol has been employed to introduce the mesogenic cholesterol unit as an end group of the polymer

Received: May 28, 2011
Revised: July 26, 2011
Published: August 12, 2011

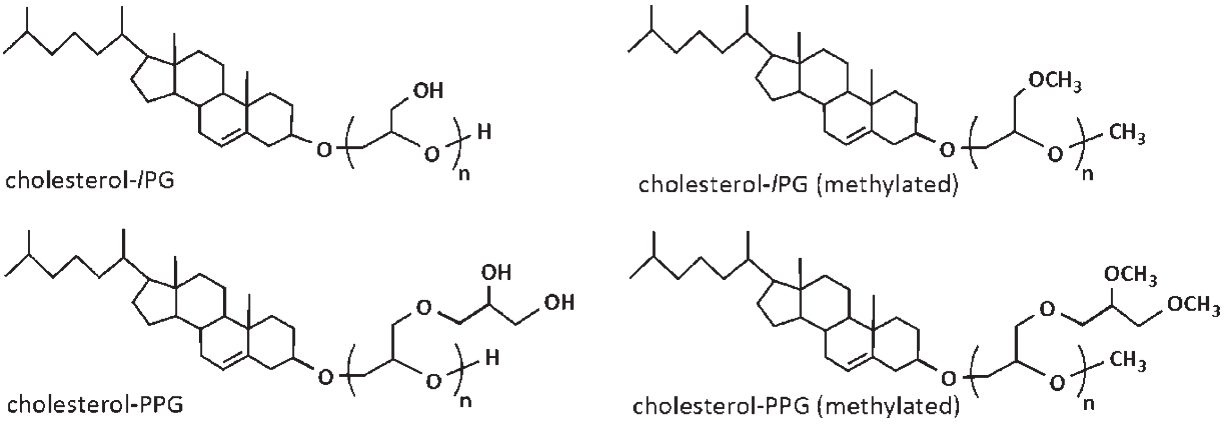

Figure 1. Chemical structures of the cholesterol-initiated polyethers before and after methylation. The respective values of the degree of polymerization *n* are given in Table 1.

structure. The central issue of this work is to which extent one single cholesterol unit can direct the structure of an otherwise isotropic, hydrophilic polymer structure. The phase behavior of the amphiphilic LC oligomers consisting both of polar, linear polyglycerols (*l*PGs) and poly(glyceryl glycerol ether)s (PGGs), respectively, and their methylated derivatives has been investigated via differential scanning calorimetry (DSC), polarized optical microscopy (POM), and small-angle X-ray scattering (SAXS).

The chemical structures of the different polyether architectures investigated in this work are shown in Figure 1. We were particularly interested in a comparison of our results to the studies of Kunieda et al.[12] and Xu et al.,[13] respectively, on structurally related rod−coil polymers consisting of cholesterol and polar (but crystallizable) PEG chains. Another related system based on rod−coil polymers of PEG and poly(propylene glycol) as flexible coils, respectively, and ethyl 4′-(4′-oxy-4-biphenylcarbonyloxy)-4-biphenylcarboxylate as a rod-like segment has been described in a series of important works by Lee et al.[37] In these works, the influence of the length of an apolar poly(propylene oxide) coil was studied in a systematic manner, keeping the rod segment constant.[37c,d]

In contrast to these previous studies, the *l*PGs employed as a coil segment in this paper are both noncrystalline and exhibit one or two functional hydroxyl groups in each monomer unit of the flexible polymer chain, which are capable of interaction via multiple hydrogen bonding. The structures may thus be considered as peculiar rod−coil topologies with a "sticky" coil architecture. We have also studied the consequences of "switching off" these hydrogen-bond interactions by full methylation of the hydroxyl groups.

EXPERIMENTAL SECTION

Instrumentation. ^{1}H nuclear magnetic resonance (NMR) spectra were recorded using a Bruker AC 300 spectrometer operated at 300 MHz, employing $CDCl_3$ and DMSO-d_6 (dimethylsulfoxide) as solvents. ^{13}C NMR spectra (referenced internally to solvent signals) were recorded at 100.15 MHz. Fourier transform infrared (FT-IR) spectra were recorded on a Nicolet iS 10 spectrometer equipped with a diamond attenuated total reflection (ATR) unit. Size exclusion chromatography (SEC) measurements were carried out in dimethylformamide (DMF) containing 0.25 g/L of lithium bromide. An Agilent 1100 Series GPC Setup (gel permeation chromatography) was used as an integrated instrument, including a Polymer Standards Service (PSS) 2-hydroxyethyl methacrylate (HEMA) column ($10^6/10^5/10^4$ g/mol) and UV (254 nm) and RI-detectors. Calibration was achieved using PEG standards provided by PSS. The eluent was used at 50 °C and at a flow rate of 1 mL/min. For SEC measurements in chloroform, a setup consisting of a Waters 717 plus autosampler, a TSP Spectra Series P 100 pump, three PSS-SDV-5 μL-columns with 100, 1000, and 10000 Å pore diameter, respectively, and a UV (275 nm) and an RI detector was used. Calibration was carried out using poly(styrene) standards provided by PSS. Matrix-assisted laser desorption and ionization time-of-flight (MALDI-TOF) measurements were performed on a Shimadzu Axima CFR MALDI-TOF mass spectrometer equipped with a nitrogen laser delivering 3 ns laser pulses at 337 nm. α-Cyano-3-hydroxycinnamic acid (CHCA) was used as matrix. Samples were prepared by dissolving the polymer in methanol at a concentration of 10 g/L. A 10 μL aliquot of this solution was added to 10 μL of a 10 g/L solution of the matrix and 1 μL of a solution of potassium trifluoroacetic acid (KTFA) (0.1 M in methanol as cationization agent). A 1 μL aliquot of the mixture was applied to a multistage target, methanol evaporated, and a thin matrix/analyte film created.

DSC measurements were carried out using a Perkin-Elmer DSC 7 with a Perkin-Elmer thermal analysis controller TAC7/DX in the temperature range of −100 to 100 °C using heating rates of 20 and 10 K/min. The melting points of indium (T_m = 156.6 °C) and Millipore water (T_m = 0 °C) were used for calibration.

POM experiments were carried out at different temperatures on an Olympus BX-51 polarized optical microscope equipped with a digital camera. A small amount of the respective sample was placed on an object plate and covered with a thin glass slide.

SAXS measurements were obtained with a system based on a conventional X-ray source for Cu Kα radiation with a wavelength λ= 0.1542 nm, an X-ray mirror, three pinholes to focus the beam, and a two-dimensional multiwire detector (Molecular Metrology). This provides an accessible range of scattering vectors $q = 4\pi/(\lambda \sin(\theta))$ from q = 0.013 Å^{-1} to q = 0.5 Å^{-1}. Beam path and sample chamber were evacuated. The sample detector distance was 75 mm. The samples were put into a sandwich of three metal discs with central holes and kapton foil to keep the sample in place. To exclude any effects of sample preparation onto the formation of the LC structures, the samples were heated over the transition temperature in the sample holder and slowly cooled down to room temperature, and the SAXS experiments were measured at 20 °C.

Reagents. All reagents and solvents were purchased from Acros and used as received, unless otherwise mentioned. Cholesterol was purchased from Fluka and stored at 4 °C. Dry solvents stored over

molecular sieves were purchased from Fluka. Deuterated $CDCl_3$ and DMSO-d_6 were purchased from Deutero GmbH, dried, and stored over molecular sieves. EEGE was prepared as described in literature using glycidol and dried over CaH_2 directly before use.[25,26,28,38] ^{1}H NMR (300 MHz, $CDCl_3$): δ (ppm) = 4.76 ($OCH(CH_3)O$), 3.35−3.90 (OCH_2CH_3 and $OCH_2C_2H_3O$), 3.15 (CH epoxide), 2.61−2.91 (CH_2 epoxide), 1.33 ($OCH(CH_3)O$), 1.19 (OCH_3). IGG was prepared as described in literature, dried over CaH_2, and freshly distilled before use.[29] ^{1}H NMR (300 MHz, CDCl3): δ (ppm) = 4.3 (CH acetal), 4.07 (CH acetal), 3.88−3.39 (OCH_2), 3.17 (CH epoxide), 2.81 (CH_2 epoxide), 1.44 (CH_3), 1.38 (CH_3).

Synthesis: Polymerization Reactions. The cholesterol-initiated rod−coil polymers were prepared in analogy to a method introduced recently.[30,31]

Cholesterol-Poly(ethoxyethyl glycidyl ether). ^{1}H NMR (300 MHz, DMSO-d_6): δ (ppm) = 5.30 (C═CH cholesterol), 4.63 (m, CHO acetal), 3.76−3.22 (polyether backbone; CHO cholesterol), 2.28−0.82 (br, CH_2, CH cholesterol), 1.17−1.06 (br, CH_3 acetal), 0.63 (br, CH_3 cholesterol). DP_n of PEEGE was determined by comparison of ma ethyl signal (0.63 ppm) of cholesterol with the signals of the acetal proton at a chemical shift of 4.63 ppm.

Deprotection to Cholesterol-Linear Polyglycerol. ^{1}H NMR (300 MHz, DMSO-d_6): δ (ppm) = 5.30 (C═CH cholesterol), 4.27 (br, OH), 3.76−3.22 (polyether backbone; CHO cholesterol), 2.28−0.82 (br, CH_2, CH cholesterol), 0.63 (br, CH_3 cholesterol).

Cholesterol-Poly(isopropylidene glyceryl glycidyl ether). ^{1}H NMR (300 MHz, DMSO-d_6): δ (ppm) = 5.30 (C═CH cholesterol), 4.14 (m, CHO acetal), 3.96 (m, CH_2O acetal), 3.76−3.22 (polyether backbone; CHO cholesterol), 2.28−0.82 (br, CH_2, CH cholesterol), 1.31−1.26 (br, CH_3 acetal), 0.63 (br, CH_3 cholesterol). DP_n of poly(isopropylidene glyceryl glycidyl ether) (PIGG) was determined by a comparison of methyl signal (0.63 ppm) of cholesterol with the signals of the PIGG at a chemical shift of 4.14 ppm.

Deprotection to Cholesterol-Poly(glyceryl glycerol ether). ^{1}H NMR (300 MHz, DMSO-d_6): δ (ppm) = 5.30 (C═CH cholesterol), 4.27 (br, OH), 3.76−3.22 (polyether backbone; CHO cholesterol), 2.28−0.82 (br, CH_2, CH cholesterol), 0.63 (br, CH_3 cholesterol).

Permethylation of the Polyether-Polyols. Permethylation of the polyether-polyols was carried out by dissolving 500 mg of the respective polymer in water (2 mL), adding sodium hydroxide to yield a 1 n solution and benzene (2 mL). Methyl iodide (10 eq. of hydroxyl groups) was added slowly via a syringe under vigorous stirring at room temperature. After additional 12 h of stirring the reaction mixture was extracted with toluene, the organic phases dried over $MgSO_4$, and the solvents were removed to obtain the methylated product in yields of about 90%.

Cholesterol-Polyglycerol (Methylated). ^{1}H NMR (300 MHz, DMSO-d_6): δ (ppm) = 5.30 (C═CH cholesterol), 3.76−3.22 (polyether backbone; CHO cholesterol), 3.23 (OCH_3), 2.28−0.82 (br, CH_2, CH cholesterol), 0.63 (br, CH_3 cholesterol).

■ RESULTS AND DISCUSSION

1. Synthesis and Characterization of Cholesterol-Polyethers. The synthesis of the cholesterol-initiated linear *l*PGs and PGGs has been carried out combining recently disclosed synthetic strategies.[26,29,31] Cholesterol has been directly used as an initiator and cesium hydroxide monohydrate as a deprotonating agent for the polymerization of different acetal-protected glycidyl derivatives. The oxyanionic ROP of EEGE initiated with commercially available cholesterol and subsequent removal of the acetal protecting groups of the PEEGE precursors under acidic conditions lead to amphiphilic linear polyglycerols with one hydroxyl function per monomer unit in the flexible coil segment.[25,26,31−35,39] In contrast the polymerization of IGG followed by acidic hydrolysis, that is, deprotection of the hydroxyl groups at the PIGG backbone, results in aliphatic polyethers bearing two additional adjacent hydroxyl groups in every PGG unit.[29,31,36] The use of cholesterol and cesium hydroxide monohydrate as an initiating system permitted good control over the molecular weights and over the degree of functionalization for the preparation of both polymers (Table 1). Nevertheless, full conversion of the initiator was not achieved during the synthesis of polymers with very low molecular weights (degree of polymerization $DP_n < 6$). This necessitated purification by precipitation of the crude products in cold diethyl ether. In this manner a series of polyether-polyols bearing one cholesterol moiety with systematically varied chain lengths as well as different polymer architectures has been prepared. By systematic alteration of both chain length and structure and thus the ratio between the lipophilic and mesogenic cholesterol and the hydrophilic, flexible polyether, the parameters governing LC behavior have been studied. In addition, the effect of the additional branching unit of PGG in comparison with the strictly linear polyglycerols has been investigated with respect to the formation of LC phases.

Incorporation of cholesterol in every polymer chain of the molecular weight distribution is crucial for the potential LC behavior of the resulting polyethers and is also expected for the living oxyanionic polymerization. Complete incorporation has been confirmed via matrix-assisted laser desorption and ionization time-of-flight (MALDI-TOF) measurements of the materials prepared (Figure 2). The controlled oxyanionic polymerization conditions lead to narrow molecular weight distributions with low polydispersity indices ($M_w/M_n < 1.2$), which have been determined via SEC in DMF using PEG standards (Figure 3). Due to the strong impact of the hydroxyl groups and the lipophilic initiator on the hydrodynamic radii of the polymers, molecular weights determined via SEC are generally underestimated, as it is obvious from the comparison with values determined from NMR. Therefore, the degree of polymerization (DP_n) was determined via ^{1}H NMR spectroscopy from the integration of the methyl group of the initiator at a chemical shift of 0.63 ppm and the acetal protecting groups at 4.63 ppm for PEEGE or rather 4.14 ppm and 3.96 ppm for PIGG. NMR spectroscopy also confirmed full conversion of the respective monomer by the disappearance of the epoxide signals at a chemical shift of 3.15 ppm and 2.61−2.91 for EEGE and at 3.17 ppm and 2.81 ppm for IGG (Figure 4). Characterization data of all polymers prepared in this study are summarized in Table 1.

With respect to their potential LC order, molecular weights of the amphiphilic polyethers were systematically varied in the range of 600−2300 g/mol, representing a DP_n of PG of 4−30. Cholesterol-initiated polyethers with chain lengths exceeding a DP_n of 26 showed no LC phases (Table 1, compound 8).

On the basis of the expectation that not only the variation of the ratio between the lipophilic, rigid cholesterol moiety and the hydrophilic, flexible polyether chain would influence the formation of LC phases, but also the introduction of further branching units in the polymer backbone, PGG chains based on IGG as the respective polyether monomer have been prepared. In addition, we were interested in the effect of amphiphilicity on mesophase formation. The impact of this parameter on LC behavior has been studied by "switching off" the polarity of the polyether chains via permethylation of the hydroxyl groups at the polymer backbone. Full methylation was achieved by use of methyl iodide in benzene/sodium hydroxide solution, as evidenced via ^{1}H NMR and infrared (IR) spectroscopy by the complete

Table 1. Characterization Data of Cholesterol-Initiated Polyglycerol and PGGs

no.	polymer	M_n (th), g/mol	M_n[a] (NMR), g/mol	M_n (SEC), g/mol	PDI[b] (SEC)	T_g (DSC), °C	I/LC transition,[d] °C
1	cholesterol-*l*PG$_4$	640	680	620[b]	1.23[b]	−38.8	160
2	cholesterol-*l*PG$_5$	760	760	630[b]	1.12[b]	−37.1	210
3	cholesterol-*l*PG$_9$	760	1050	690[b]	1.10[b]	−28.8	250
4	cholesterol-*l*PG$_{10}$	1050	1130	770[b]	1.09[b]	−25.8	260
5	cholesterol-*l*PG$_{12}$	1200	1280	940[b]	1.07[b]	−25.0	170
6	cholesterol-*l*PG$_{16}$	1420	1570	1090[b]	1.10[b]	−17.2	190
7	cholesterol-*l*PG$_{26}$	2240	2310	1360[b]	1.25[b]	−14.1	120
8	cholesterol-*l*PG$_{30}$	2460	2610	1480[b]	1.27[b]	−10.2	
9	cholesterol-PGG$_4$	830	980	840[b]	1.15[b]	−49.8	
10	cholesterol-PGG$_7$	1220	1420	980[b]	1.21[b]	−49.5	
11	cholesterol-PGG$_9$	1470	1720	1080[b]	1.08[b]	−33.9	
12	cholesterol-PGG$_{13}$	2290	2320	1240[b]	1.17[b]	−41.3	
13	cholesterol-*l*PG$_4$ (methylated)	750	750	640[b]	1.27[b]	−81.6	
				930[c]	1.75[c]		
14	cholesterol-*l*PG$_5$ (methylated)	840	840	650[b]	1.18[b]	−65.5	5
				980[c]	1.17[c]		
15	cholesterol-*l*PG$_9$ (methylated)	1190	1190	590[b]	1.09[b]	−66.3	25
				720[c]	1.23[c]		
16	cholesterol-*l*PG$_{10}$ (methylated)	1280	1280	750[b]	1.08[b]	−74.0	35
				1000[c]	1.23[c]		
17	cholesterol-*l*PG$_{12}$ (methylated)	1460	1460	910[b]	1.17[b]	−66.3	
				1270[c]	1.17[c]		
18	cholesterol-*l*PG$_{16}$ (methylated)	1810	1810	940[b]	1.06[b]	−67.7	
				1650[c]	1.23[c]		
19	cholesterol-PGG$_4$ (methylated)	1110	1110	900[b]	1.07[b]	−77.1	
				1400[c]	1.16[c]		
20	cholesterol-PGG$_7$ (methylated)	1630	1630	920[b]	1.21[b]	−75.9	
				1550[c]	1.44[c]		
21	cholesterol-PGG$_9$ (methylated)	1990	1990	990[b]	1.20[b]	−73.8	
				1820[c]	1.23[c]		
22	cholesterol-PGG$_{13}$ (methylated)	2700	2700	1200[b]	1.10[b]	−71.9	
				2170[c]	1.25[c]		

[a] M_n determined via ^{1}H NMR spectroscopy. [b] M_n and M_w determined via SEC-RI in DMF with PEG standards. [c] M_n and M_w determined via SEC-RI in $CHCl_3$ with poly(styrene) standards. [d] Isotropic/liquid crystal transition temperature determined via POM.

disappearance of the signals at a chemical shift of 4.27 ppm or respectively at a wavenumber of 3200−3550 cm^{-1} (Figures 4 and 5). In contrast to the amphiphilic cholesterol PGs, the permethylated samples exhibit good solubility in apolar solvents and $CHCl_3$, as expected.

As it is clearly confirmed by the above-mentioned characterization methods (SEC, NMR, MALDI-TOF), two series of cholesterol-initiated oligo- and polyglycerols with different molecular architectures have been obtained via the oxyanionic ROP of EEGE and IGG and subsequent acidic removal of the acetal protecting groups. To study fully hydrophobic materials that exhibit no amphiphilic character, permethylation of the polyethers has been carried out, using methyl iodide. The successful transformation has been confirmed via NMR and IR spectroscopy.

2. Thermal and Optical Characterization of the Cholesterol-Polyethers. Central issues in the context of the current study are: (i) up to which chain length can an isotropic, hydrophilic polymer structure still be ordered in an LC structure by a single cholesterol mesogen at the chain end and (ii) what is the influence of the structure and polarity of the flexible chain on LC order? The materials studied may either be considered as rod−coil polymers with a small, rigid unit and a "sticky" coil segment or as single-mesogen terminated isotropic and flexible polymer liquids at room temperature. In comparison to previous works on rod−coil structures with poly(ethylene oxide) (PEO) or poly(propylene oxide) (PPO) chains, the materials discussed in this paper are of a different nature, since they cannot crystallize like PEO and possess a highly polar, isotropic structure in contrast to PPO.[37c,d]

Since the formation of LC phases of amphiphilic polymers is often induced by segregation of the incompatible chain ends, the thermotropic behavior of the cholesterol-initiated polyethers will most probably depend on their amphiphilicity and the phase separation of hydrophilic polymer chain and the hydrophobic cholesterol.[6,12,13,37,40−48] To this end, the structure of the polyglycerols has been transformed via permethylation of the hydroxyl groups at the polymer backbone, resulting in an apolar coil structure.

The thermotropic LC behavior of the amphiphilic polyglycerols with different polymer architectures and chain lengths (Table 1) has been investigated via POM and DSC. The glass

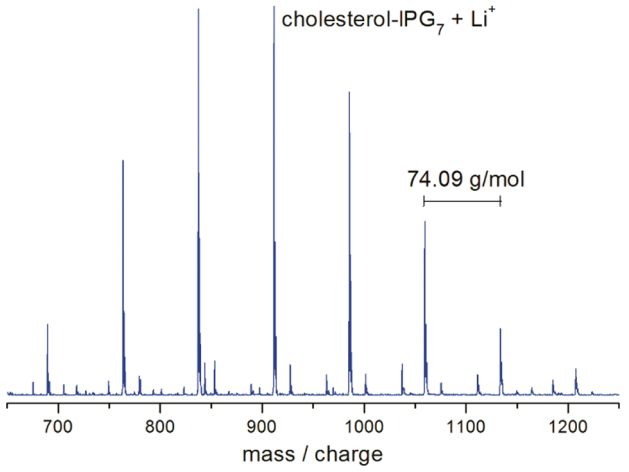

Figure 2. Typical MALDI-TOF of linear polyglycerol (cf. compound 4, Table 1), initiated with cholesterol. The main distribution is obtained with lithium as a counterion; the subdistribution is due to sodium as a counterion. The attachment of cholesterol to all polyether chains is confirmed.

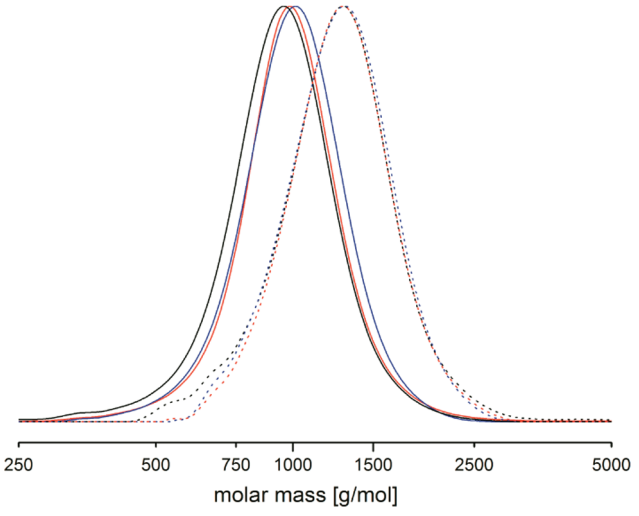

Figure 3. SEC measurements (DMF) of linear polyglycerols with different molecular weights before (solid lines) and after removal of the acetal protecting groups (dotted lines). Black: cholesterol-PEEGE$_{10}$, cholesterol-*l*PG$_{10}$ (cf. compound 4, Table 1). Red: cholesterol-PEEGE$_{12}$, cholesterol-*l*PG$_{12}$ (cf. compound 5, Table 1). Blue: cholesterol-PEEGE$_{16}$, cholesterol-*l*PG$_{16}$ (cf. compound 6, Table 1).

transition temperatures (T_g) of the cholesterol-initiated polyethers determined by DSC measurements range from −20 to −50 °C, depending on their structure and their chain lengths (Table 1). Especially in the series of linear polyglycerols, a clear correlation of T_g with the degree of polymerization has been observed; that is, the glass transition temperatures systematically vary from −39 °C for cholesterol-*l*PG$_4$, −37 °C for cholesterol-*l*PG$_5$, −29 °C for cholesterol-*l*PG$_9$, −26 °C for cholesterol-*l*PG$_{10}$, and −25 °C for cholesterol-*l*PG$_{12}$ to −17 °C for cholesterol-*l*PG$_{16}$. This tendency reflects the higher chain mobility of lower molar mass chains and the increasing influence of hydrogen bonds of the hydroxyl functional polymers. In contrast, PGGs with different molecular weights showed transition temperatures in the range of −50 °C to −33 °C without

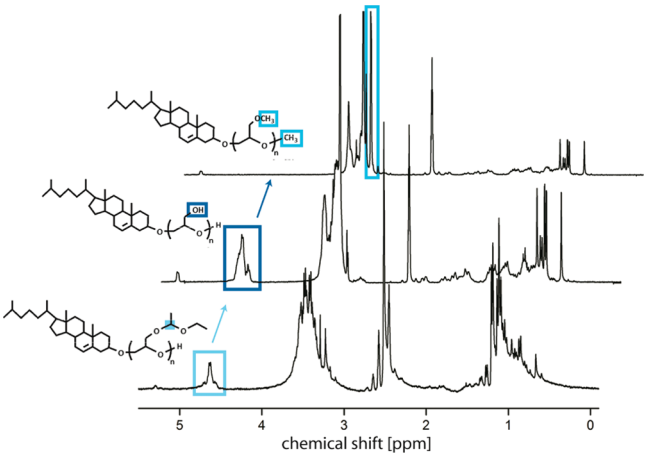

Figure 4. ^{1}H NMR spectra of linear cholesterol-PEEGE, cholesterol-*l*PG (bottom, cf. compound 4, Table 1), and methylated *l*PG-OMe (top spectrum, compound 14, Table 1) measured in DMSO-d_6.

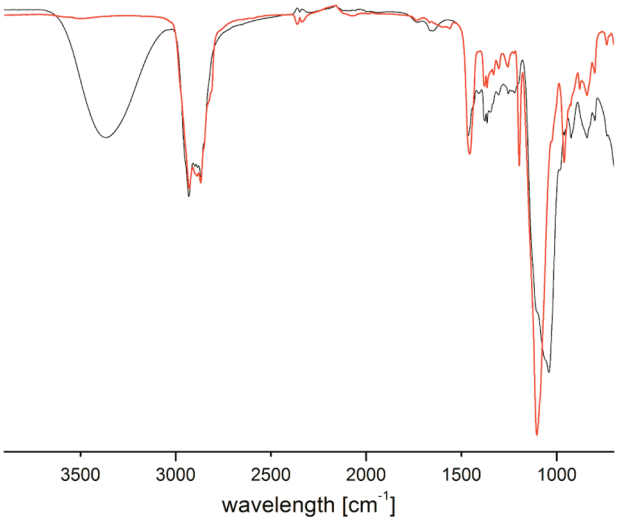

Figure 5. IR spectrum of linear polyglycerol (black, cf. compound 2, Table 1) and methylated *l*PG (red, cf. compound 12, Table 1). The disappearance of the band at 3500 cm^{-1} confirms full methylation.

clear dependence on molecular weights. Full methylation of the polyether-polyols generally leads to strongly lowered T_g's, varying from −82 °C to −66 °C due to the absence of polar hydroxyl groups that restrict mobility of the polyether chains by the formation of hydrogen bonds.

An investigation of the amphiphilic polymers with POM revealed LC phases for all linear polyglycerols presented in this study up to a DP$_n$ of 26 within a broad temperature range (Figure 6). Since the glass transition temperatures of the cholesterol-*l*PGs vary from −20 °C to −40 °C, the birefringence observed via POM between crossed polarizers at higher temperatures resulted from anisotropic fluids, evidencing the presence of LC phases. At temperatures below the T_g's of the cholesterol-initiated polyglycerols the birefringence was caused by vitrification of the LC-phase to an anisotropic glass. Although no further phase transitions were observed via DSC, different LC phases have been observed with POM before isotropization. With increasing chain length the temperatures for the LC/isotropic

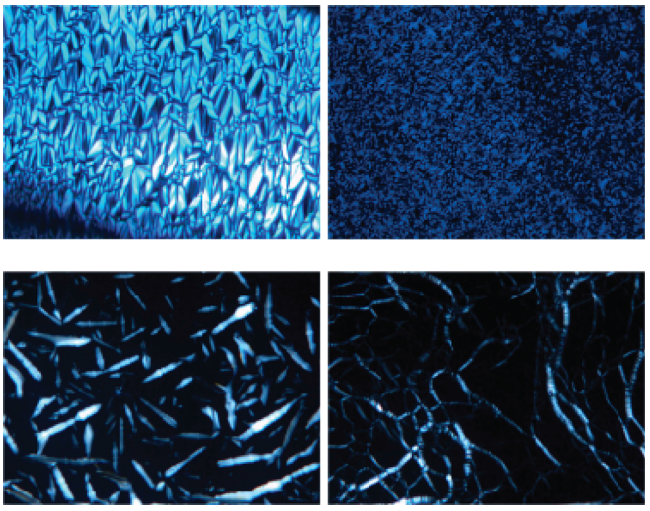

Figure 6. Optical textures of cholesterol-*l*PG observed with the polarizing microscope at different temperatures (crossed polarizers): POM micrographs of cholesterol-*l*PG_{16} (cf. compound 6, Table 1) at 160 °C (top, left) and 100 °C (top, right) and of cholesterol-*l*PG_{10} (cf. compound 12, Table 1) at 255 °C (bottom, left) and 180 °C (bottom, right).

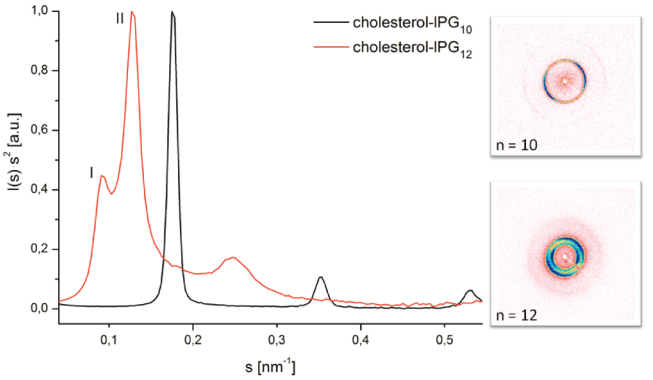

Figure 7. Left: SAXS profiles of cholesterol-*l*PG_{10} (black) and cholesterol-*l*PG_{12} (red) measured at 20 °C. Right: 2D SAXS images of cholesterol-*l*PG_{10} (top) and cholesterol-*l*PG_{12} (bottom).

transitions of the amphiphilic polyglycerols rise from 160 °C for cholesterol-*l*PG_4, 210 °C for cholesterol-*l*PG_5, and 250 °C for cholesterol-*l*PG_9 to 260 °C for cholesterol-*l*PG_{10}. This is explained by the increasing number of interacting hydroxyl groups.

Polymers with higher molecular weights showed lower transition temperatures, that is, 170 °C for cholesterol-*l*PG_{12}, 190 °C for cholesterol-*l*PG_{16}, and 120 °C for cholesterol-*l*PG_{26}. POM revealed well-developed optical textures, including smectic A (SmA) bâtonnets (crystalline sticks) on cooling from the isotropic melt of all cholesterol-*l*PGs presented in this study, suggesting the formation of SmA phases due to microphase separation of the hydrophobic cholesterol and the hydrophilic polyether chain (Figure 6). For polyglycerols with a degree of polymerization exceeding 26 glycerol units, no birefringence has been observed with POM. At lower temperatures, that is, 150 °C for cholesterol-*l*PG_{16} (cf. compound 6, Table 1), the formation of fan-like textures similar to twist grain boundary A (TGBA) phases has been observed. This is in good agreement with theoretical considerations as well as results from SAXS experiments discussed in the following. The driving forces for LC order in this type of polymers may on one hand be the amphiphilicity of the cholesterol-polyglycerols, leading to nanosegregation in layered structures, such as SmA phases. On the other hand cholesterol tends to form chiral nematic or cholesteric phases.[49] The incompatibility of the twist observed in the cholesteric phase with the layered structure of the SmA phase presumably results in a frustrated structure similar to TGBA phases. The formation of oily streaks on cooling from the isotropic melt has been observed only in one compound, namely, cholesterol-*l*PG_{10}, at 180 °C, while further cooling leads to the formation of SmA phases in analogy to the phase behavior of the related compounds.

Comparing our results to the studies of Lee et al. on the three-dimensional supramolecular organization of molecular rods depending on the coil cross section,[37] the formation of lamellar phases of the cholesterol-initiated polyglycerols is in good agreement with the results for the LC behavior of PEG and PPO rod−coil oligomers with ABA structures.[50,51] However, the investigated polymers as well as the employed mesogens, that is, biphenyl compounds, presented by Lee et al. only permit a limited comparison with the cholesterol-*l*PGs with different cross sections and hydroxyl functionality. Compared to our results, cholesteryl end-capped PEGs reported by Xu et al. in 2006[13] self-assemble in layered LC phases up to a degree of polymerization of n = 25−30, where the mesogenic cholesterol moiety loses its influence on the superstructure of the polymer due to the dominating crystallization of the PEG chain.[13] In contrast to these cholesterol-PEGs, where thermotropic behavior of the materials strongly depends not only on their amphiphilic character but also on the formation of spherulites, linear cholesterol-initiated polyglycerols are unable to crystallize due to their atactic structure. However, the influence of the additional hydroxyl functions at the polyether backbone distinguishes the herein presented complex polymers from previously studied systems.

Since amphiphilicity of the polyglycerols appears to be an important driving force for the formation of LC phases, methylation of the hydroxyl functionalities was expected to give insight into the significance of the interplay of flexibility and rigidity for mesophase formation by "switching off" the amphiphilic nature. It is obvious from the data compiled in Table 1 (samples 13−22) that permethylation of the polymer backbone lead to strongly reduced stability of the LC order. Only the methylated polyglycerol samples 14−16 with a degree of polymerization between 5 and 10 glycerol units showed LC order in this case. For all samples permethylation generally resulted in strongly reduced viscosity and glass transitions between −65 and −82 °C, that is, 40 K lower than for the hydroxyl-functional samples. In the case of the LC samples 14−16 isotropization occurred already at fairly low temperatures between 5 and 35 °C. Thus, the temperature regime for the existence of LC order was considerably narrower than in the original samples, confirming the important role of an amphiphilic structure and hydrogen bonding of the polar segment for the stabilization of the LC phases. For samples with shorter or longer methylated oligoglycerol segments the mesophases vanished completely upon methylation. We conclude that strong immiscibility leading to phase segregation represents the major driving force for LC order in these systems.

3. SAXS Measurements of Cholesterol-Polyethers. The presence of domain ordering was investigated by SAXS measurements at 20 °C. In Figure 7 we present two typical examples of the scattering patterns. The two-dimensional pattern clearly shows a partial orientation of the domains. Taking the azimuthal

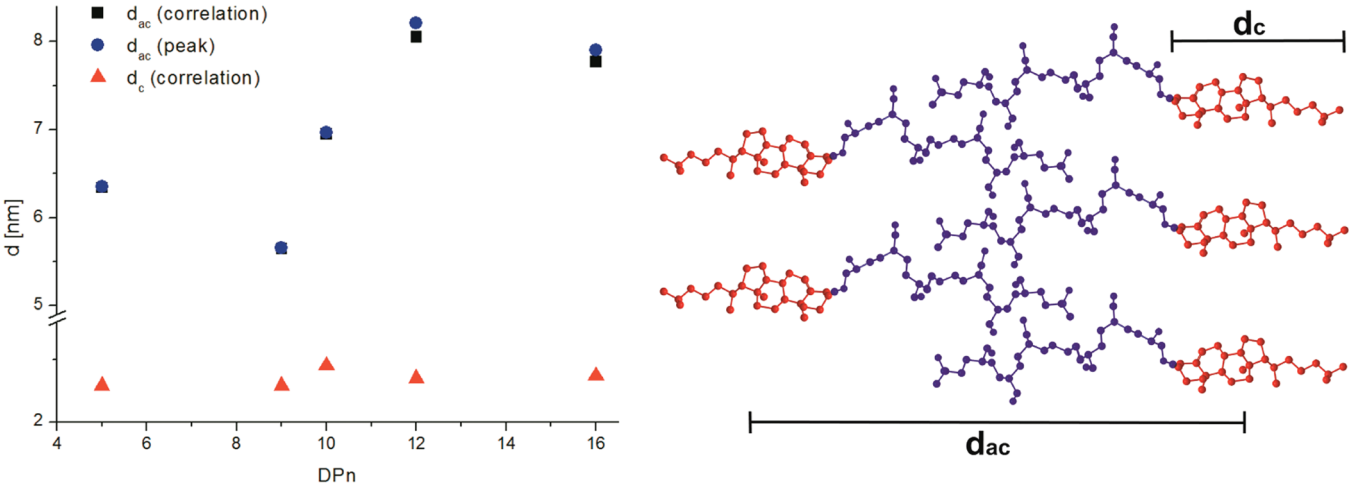

Figure 8. Left: Layer thickness obtained via SAXS measurements (peaks and correlation function) vs chain length of cholesterol-initiated polyglycerols. Right: Packing model for the amphiphilic polyglycerols with rigid cholesterol end groups and flexible polyether chains.

average, we arrive at the intensity in dependence on $s = (2/\lambda)\sin\theta$ with 2θ being the scattering angle shown in the left part of the figure. For $n = 12$, two series of reflections can be discriminated. Their lowest order reflection is labeled I and II in Figure 7. They are related to differently oriented domains as can be seen in the two-dimensional intensity distribution. The higher order reflections of series I are apparently of low intensity and covered by the strong reflections of series II:

Sample 4 (lPG$_{10}$) displays only one series of reflections with three narrow peaks indicative of a well-formed lamellar structure. Also the intensity distribution only displays one dominant domain orientation.

In the following we discuss the variation of the lamellar structure with molecular weight. For samples lPG$_{10}$ and lPG$_{12}$, this refers to the reflection series II in Figure 7. The s value of the first order reflection is directly related to the period of the structure $d = 1/s$. To characterize the lamellar structure in more detail, we calculated the linear correlation function. This allows to determine not only the period of the lamellar structure but also the thickness of the cholesterol and PG domains separately.[52] In parallel we use the position of the peaks shown in Figure 7 to calculate the period of the lamellar structure d. Linear cholesterol-initiated polyglycerols showed several characteristic diffraction peaks, suggesting the presence of lamellar phases (Figure 7). Thus, a minimum of two clear peaks at $s_1 = 1/d$ and $s_2 = 2/d$ are observed for cholesterol-lPGs with degrees of polymerization of n = 5, 9, 10, 12, and 16, indicating the formation of layered structures in all amphiphilic linear polyglycerols presented in this study. Additionally, SAXS measurements revealed an increase of the layer thicknesses with increasing chain lengths of the cholesterol-modified polyethers, whereas similar values in a range of d_c = 2.3−2.5 nm are obtained for the rigid cholesterol moiety. Its length is constant in all scattering experiments (Figure 8). Thus, the layer spacing varies from d_{ac} = 6.3 nm for cholesterol-lPG$_5$ to d_{ac} = 7.0 nm for cholesterol-lPG$_{10}$ and d_{ac} = 8.1 nm for cholesterol-lPG$_{12}$ (Figure 8). Small variations in this trend might be related to the closer packing of polymers in layered structures with increasing DP$_n$ due to higher overlap of alternating polymer chains. Nevertheless, the values of the layer thickness are in good accordance with theoretical considerations, that is, comparing these structures to analogous PEG-containing LCs. Therefore, a single layered structure of the polyether chains is most likely formed, while the rigid cholesterol end groups are packed in double-layered conformations (Figure 8).

As mentioned above, in cholesterol-polyglycerols with higher molecular weights, two types of structure with varying layer spacing were identified by SAXS measurements (Figure 7). Assuming the reflection labeled I in Figure 7 to be the first order of a lamellar series layer thicknesses of d_{ac}' = 10.9 nm were obtained for cholesterol-lPG$_{12}$ and d_{ac}' = 13.7 nm for cholesterol-lPG$_{16}$. The presence of different lamellar phases might result from varying overlap of the polyether chains due to diverse chain lengths, which is more pronounced in polymers with higher DP$_n$. The observed thickness indeed fits well with the assumption of overlapping polyether chains. The different structures may also derive from the incompatibility of the chiral nematic ordering of cholesterol with the lamellar ordering of amphiphiles, leading to frustrated layered phases which are tilted to each other.

Analogous measurements with cholesteryl end-capped PEGs revealed layer thicknesses of 5.1 nm for n = 5−9.3 nm for n = 20 and similar packing models.[13] However, in contrast to these previous studies on the self-assembly of cholesterol-PEGs, where the layer spacing also depends on the crystallization of the PEG chain, leading to the coexistence of different lamellar structures due to nearly amorphous LC or crystalline phases, the linear cholesterol-initiated PGs are unable to crystallize. The amorphous, flexible polyether chains of cholesterol-PGs allow good overlap in spite of their spatially demanding hydroxyl groups at the polymer backbone. On the other hand, the presence of hydrogen bonds between the closely packed polymer chains and the highly amphiphilic character of the materials actually results in very stable LC order in a very broad temperature range up to 260 °C, while analogous cholesterol-PEGs exhibit LC ordering only up to 100 °C.[12] Since the enhanced stability of the LC order by higher amphiphilicity is limited by sterical constraints, PGGs with comparable molecular weights exhibit no LC behavior (Table 1).

CONCLUSION

We have studied the synthesis and thermal properties of linear polyglycerol (PG) and PGG, functionalized with one single

mesogenic cholesterol unit. This was achieved by using cholesterol directly as an initiator for the oxyanionic ROP of the respective epoxide monomers, that is, EEGE and IGG. The resulting linear polyglycerols showed LC order in an extremely broad temperature range up to 260 °C. POM and SAXS experiments revealed self-assembly of the linear, cholesterol-initiated polyglycerols in layered phases with varying layer thicknesses in the range of 5.7−8.1 nm, depending on the chain lengths of the respective polymer up to a degree of polymerization (DP_n) of 26. This demonstrates the strong structure-directing effect of the single cholesterol unit, forcing an isotropic liquid, highly polar polymer structure into an ordered mesophase state.

The formation of LC phases in cholesterol-initiated polyglycerols is controlled by three main parameters: (i) by the ratio between the hydrophobic mesogen at the chain end and the hydrophilic polyether moiety; (ii) by the molecular architecture of the respective monomer, that is, linear glycerol moieties or branched glyceryl glycerol units, (iii) by the hydroxyl functionalities at the polymer chain, contributing to the hydrophilicity and the generation of strong intermolecular interactions. The thermotropic behavior of cholesterol-modified PEG depends on the crystallization of the PEG chains, which becomes more relevant with increasing chain length.[13] Since linear polyglycerols and PGGs show no crystallization and the amphiphilic character is more distinct in these polymers due to the multiple hydroxyl groups at the polyether backbone, highly stable LC order is observed in comparison to the structurally related cholesterol-PEGs and previously studied rod−coil structures consisting of extended rods with biphenyl structures and PEO or PPO coils.[37c,d] Hydrogen bonds between the polymer chains in the layered structures stabilize LC order in a very broad temperature range up to 260 °C, while the analogous cholesterol-PEGs exhibit LC ordering only up to 100 °C.[12] From this study it is obvious that the formation of LC phases depends on one hand on the amphiphilicity of the polymers, but on the other hand is limited by steric constraints, PGGs with comparable molecular weights showed no LC order.

Given their convenient availability in a single step and their biocompatibility, the LC cholesterol-initiated polyglycerols are promising for structured hydrogels, lyotropic LC hydrogels or novel types of hybrid materials by combination with inorganic components. In this context, we are presently investigating to which extent the highly stable mesophases are affected by partial functional transformation of the hydroxyl groups of PG.

■ ASSOCIATED CONTENT

Supporting Information. Additional MALDI-TOF characterization data (Figures S1−S3). This material is available free of charge via the Internet at http://pubs.acs.org.

■ AUTHOR INFORMATION

Corresponding Author

*E-mail: hfrey@uni-mainz.de.

■ ACKNOWLEDGMENT

We thank Prof. Rudolf Zentel for valuable discussions. We are grateful to Dr. Florian Wolf for MALDI-TOF measurements. Furthermore, the authors thank Daniel Loeper and Eric Hoffmann for their valuable technical assistance. A.M.H. is a recipient of a fellowship of the Graduate School of Excellence MAINZ (Materials Science in Mainz) through funding of the Excellence Initiative (DFG/GSC 266).

■ REFERENCES

(1) Reinitzer, F. *Monatsh. Chem.* **1888**, *9*, 421–441.
(2) Marcos, M.; Martin-Rapun, R.; Omenat, A.; Serrano, J. L. *Chem. Soc. Rev.* **2007**, *36*, 1889–1901.
(3) Imrie, C. T.; Henderson, P. A. *Chem. Soc. Rev.* **2007**, *36*, 2096–2124.
(4) Zhou, Y.; Briand, V. A.; Sharma, N.; Ahn, S.-K.; Kasi, R. M. *Materials* **2009**, *2*, 636–660.
(5) Donnio, B.; Guillon, D. *Adv. Polym. Sci.* **2006**, *201*, 45–155.
(6) Tschierske, C. *J. Mater. Chem.* **1998**, *8* (7), 1485–1508.
(7) Schlüter, A. D.; Rabe, J. P. *Angew. Chem., Int. Ed.* **2000**, *39*, 864–883.
(8) Meier, H.; Lehmann, M. *Angew. Chem., Int. Ed.* **1998**, *37*, 643–645.
(9) Cameron, J. H.; Facher, A.; Lattermann, G.; Diele, S. *Adv. Mater.* **1997**, *9*, 398–403.
(10) Barberá, J.; Donnio, B.; Gehringer, L.; Guillon, D.; Marcos, M.; Omenat, A.; Serrano, J. L. *J. Mater. Chem.* **2005**, *15*, 4093–4105.
(11) Bosman, A. W.; Janssen, H.; Meijer, E. W. *Chem. Rev.* **1999**, *99*, 1665–1688.
(12) Lopez-Quintela, M. A.; Akahane, A.; Rodriguez, C.; Kunieda, H. *J. Colloid Interface Sci.* **2002**, *247*, 186–192.
(13) Xu, J.-T.; Xue, L.; Fan, Z.-Q.; Wu, Z.-H.; Kim, J. K. *Macromolecules* **2006**, *39*, 2981–2988.
(14) Sunder, A.; Quincy, M. F.; Mülhaupt, R.; Frey, H. *Angew. Chem., Int. Ed.* **1999**, *38*, 2928–2930.
(15) Zhang, X.; Chen, Y.; Gong, A.; Chen, C.; Xi, F. *Liq. Cryst.* **1998**, *25*, 767–769.
(16) Quincy, M. F.; Kautz, H.; Frey, H. *Polym. Mater. Sci. Eng.* **2001**, *84*, 647–648.
(17) Nagahama, K.; Ueda, Y.; Ouchi, T.; Ohya, Y. *Biomacromolecules* **2007**, 3938–3943.
(18) Kaneko, T.; Nagasawa, H.; Gong, J. P.; Osada, Y. *Macromolecules* **2004**, *37*, 187–191.
(19) Hartwig, A.; Mahato, T. K.; Kaese, T.; Wöhrle, D. *Macromol. Chem. Phys.* **2005**, *206*, 1718–1730.
(20) Zhou, Y.; Kasi, R. M. *J. Polym. Sci., Part A: Polym. Chem.* **2008**, *46*, 6801–6809.
(21) Klok, H. A.; Hwang, J.; Iyer, S.; Stupp, S. *Macromolecules* **2002**, *35*, 746–759.
(22) Zhou, T.; Li, F.; Cheng, S. X.; Zhuo, R. X. *J. Biomater. Sci., Polym. Ed.* **2006**, *17*, 1093–1106.
(23) Zhang, L.; Wang, Q. R.; Jiang, X. S.; Zhuo, R. X. *J. Biomater. Sci., Polym. Ed.* **2005**, *16*, 1095–1108.
(24) Zou, T.; Cheng, S. X.; Zhuo, R. X. *Colloid Polym. Sci.* **2005**, *283*, 1091–1099.
(25) Lapienis, G.; Penczek, S. *Biomacromolecules* **2005**, *6*, 752–762.
(26) Wurm, F.; Nieberle, J.; Frey, H. *Macromolecules* **2008**, *41*, 1184–1188.
(27) Dworak, A.; Baran, G.; Trzebicka, B.; Walach, W. *React. Funct. Polym.* **1999**, *42* (1), 31–36.
(28) Dimitrov, P.; Utrata-Wesolek, A.; Rangelov, S.; Walach, W.; Trzebicka, B.; Dworak, A. *Polymer* **2006**, *47*, 4905–4915.
(29) Wurm, F.; Nieberle, J.; Frey, H. *Macromolecules* **2008**, *41*, 1909–1911.
(30) Hofmann, A. M.; Wurm, F.; Hühn, E.; Nawroth, T.; Langguth, P.; Frey, H. *Biomacromolecules* **2010**, 568–574.
(31) Hofmann, A. M.; Wurm, F.; Frey, H. *Macromolecules* **2011**, *44*, 4648–4657.
(32) Mangold, C.; Wurm, F.; Obermeier, B.; Frey, H. *Macromol. Rapid Commun.* **2010**, *31*, 258–264.

(33) Eberich, M.; Keul, H.; Möller, M. *Macromolecules* **2007**, *40*, 3070–3079.
(34) Halacheva, S.; Rangelov, S.; Tsvetanov, C. B. *Macromolecules* **2006**, *39*, 6845–6852.
(35) Dimitrov, P.; Rangelov, S.; Dworak, A.; Haraguchi, N.; Hirao, A.; Tsvetanov, C. B. *Macromol. Symp.* **2004**, *215*, 127–139.
(36) Mangold, C.; Wurm, F.; Obermeier, B.; Frey, H. *Macromolecules* **2010**, *43*, 8511–8518.
(37) (a) Lee, M.; Oh, N.-K. *J. Mater. Chem.* **1996**, *6*, 1079–1086. (b) Lee, M.; Oh, N.-K.; Zin., W.-C. *Chem. Commun.* **1996**, 1787–1788. (c) Lee, M.; Cho., B.-K.; Kim, H.; Zin, W.-C. *Angew. Chem., Int. Ed.* **1998**, *37*, 638–640. (d) Lee, M.; Cho, B.-K.; Kim, H.; Yoon, J.-Y.; Zin, W.-C. *J. Am. Chem. Soc.* **1998**, *120*, 9168–9179.
(38) Dworak, A.; Baran, G.; Trzebicka, B.; Walach, W. *React. Funct. Polym.* **1999**, *42*, 31–36.
(39) Taton, D.; Borgne, A. L.; Sepulchre, M.; Spassky, N. *Macromol. Chem. Phys.* **1994**, *195*, 139.
(40) Förster, S.; Plantenberg, T. *Angew. Chem., Int. Ed.* **2002**, *41*, 689–694.
(41) Loo, Y. L.; Register, R. A.; Ryan, A. *Macromolecules* **2002**, *35*, 2365–2374.
(42) Fischer, H.; Poser, S.; Arnold, M. *Liq. Cryst.* **1995**, *18*, 503–508.
(43) Schneider, A.; Zanna, J. J.; Yamada, M.; Finkelmann, H.; Thomann, R. *Macromolecules* **2000**, *33*, 649–651.
(44) Abeysekera, R.; Bushby, R. J.; Caillet, C.; Hamley, I. W.; Lozman, O. R.; Lu, Z. B.; Robards, A. W. *Macromolecules* **2003**, *36*, 1526–1533.
(45) Ansari, I. A.; Castelletto, V.; Mykhaylyk, T.; Hamley, I. W.; Lu, Z. B.; Itoh, T.; Imrie, C. T. *Macromolecules* **2003**, *36*, 8898–8901.
(46) Yi, Y.; Fan, X. H.; Wan, X. H.; Li, L.; Zhao, N.; Chen, X. F.; Xu, J.; Zhou, Q. F. *Macromolecules* **2004**, *37*, 7610–7618.
(47) Li, C. Y.; Tenneti, K. K.; Zhang, D.; Zhang, H. L.; Wan, X. H.; Chen, E. Q.; Zhou, Q. F.; Carlos, A. O.; Igos, S.; Hsiao, B. S. *Macromolecules* **2004**, *37*, 2854–2860.
(48) Tschierske, C. *Curr. Opin. Colloid Interface Sci.* **2002**, *7*, 355–370.
(49) Goodbye, J. W. *Curr. Opin. Colloid Interface Sci.* **2002**, *7*, 326–332.
(50) Cho, B.-K.; Chung, Y.-W.; Lee, M. *Macromolecules* **2005**, *38*, 10261–10265.
(51) Lee, M.; Cho, B.-K.; Zin, W.-C. *Chem. Rev.* **2001**, *101*, 3869–3892.
(52) Ivanova, R.; Staneva, R.; Geppert, S.; Heck, B.; Walter, B.; Gronski, W.; Stühn, B. *Colloid Polym. Sci.* **2004**, *282*, 810–824.